A Novel Reference Current Calculation Method for Shunt Active Power Filters using a Recursive Algebraic Approach

H. R. Imani jajarmi[1], A. Mohamed[2] and H. Shareef [3]
[1, 2, 3]Department of Electrical, Electronic & Systems Engineering
University Kebangsaan Malaysia, Malaysia
Email: imani145@gmail.com
.

ABSTRACT
This paper presents a novel method to calculate the reference source current and the reference compensating current for shunt active power filters (SAPFs). This method first calculates the amplitude and phase of the fundamental load current from a recursive algebraic approach block before calculating the displacement power factor. Next, the amplitude of the reference mains current is computed with the corresponding phase voltage. Finally, the difference between the actual load current and the reference source current is considered the reference compensating current to be delivered by the SAPF. The proposed method is presented and applied to the control system of the voltage source converter of SAPFs. The performance of the proposed method in reducing harmonics and improving the power factor is examined with a SAPF simulation model. The results are compared with the instantaneous active and reactive p-q power theory as other reference generation method.

KEYWORDS: power quality, p-q theory, recursive algebraic approach, reference source current, shunt active power filter

1. INTRODUCTION

The result of industrial development and widespread use of power electronics is the increasing effects of harmonics on power systems. The use of non-linear loads such as electronic power supplies, rectifiers, and static power converters is the main factor of harmonic current generation. Most of these non-linear loads contribute also to lower power factor, reactive power burden, unbalance, and other problems that lead to low system efficiency and create serious power quality problems.

Among the miscellaneous options available for the improvement of power quality, the use of active power filters (APFs) is greatly accepted and employed as a significant option in power distribution systems to compensate current and voltage perturbations [1–2]. By using a control strategy, APF generates suitable compensating voltage/current signals that cancel the reactive power and harmonic components in the voltage/currents from the mains. The control strategy for the shunt active power filter (SAPF) comprises of reference signal extraction, control of DC capacitor voltage, and switching signal generation. The extraction of compensating current/voltage reference from the distorted

and harmonic polluted current/voltage signals forms the basis of the control strategy in the SAPF. Prior to calculating the reference source current and the reference compensating current, harmonics from the current signals have to be first detected. Harmonic current detection techniques are classified into time-based and frequency-based techniques. Some of the most commonly used techniques are described as follows.

The frequency-based techniques include conventional Fourier and fast Fourier transform algorithms [3], modified Fourier series techniques [4], discrete Fourier transform [5], and recursive discrete Fourier transform [6]. The time-based techniques include the dq method [3], instantaneous active and reactive p-q power theory [7], the synchronous detection method [8], and synchronous reference frame theory [9].

In this paper, the proposed method for calculating the reference current is compared with the popular instantaneous active and reactive p-q power theory. The simulation results were presented to compare the effectiveness of both algorithms.

2. SHUNT ACTIVE POWER FILTER

2.1. Basic compensation principle

Fig. 1 shows schematic diagram of SAPF [10], which is controlled to supply a compensating current at the point of common coupling (PCC) and to cancel current harmonics on the supply side.

The SAPF is controlled to draw/supply a compensated current from/to the utility to facilitate the elimination of harmonic and reactive currents of the non-linear load.

In order for the resulting total current drawn from the AC mains is sinusoidal, the SAPF should generate sufficient appropriate compensating current.

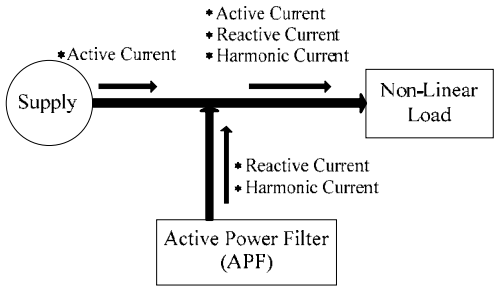

Fig. 1. Connection of SAPF with non-linear load

2.2. Reference source currents

The control strategy of SAPF generates the reference current (if). The reference source current generation should be conducted correctly for optimal compensation. This current must be provided by the active power filter to compensate for reactive power and harmonic currents demanded by the load as described in Fig. 2.

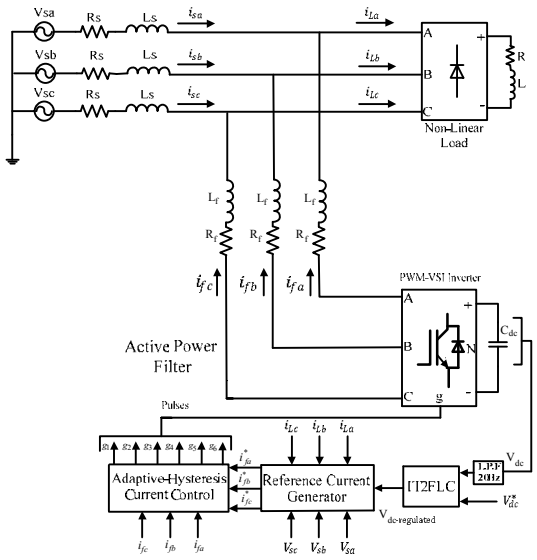

Fig. 2. Closed-loop fuzzy logic-controlled SAPF

3. PROPOSED ALGEBRAIC APPROACH TO HARMONICS CALCULATION

A sampled form of a power signal with harmonics is generally represented by the

following equation [11]:

$$x(k) = x_0 + \sum_{n=1}^{N} A_n \cos(2\pi nf_\circ T_s k + \varphi_n) \quad (1)$$

where x_0, n, N, f_o, T_s, k, and φ_n are the DC component, number of harmonics, number of last harmonic, signal frequency, sampling period, number of samples, and phase of the nth harmonic, respectively. $x(k)$ is the sampled value of the signal in the k[th] sequence. $x(k)$ can be written as follows [11]:

$$x(k) = x_0 + \sum_{n=1}^{N} \left[a_n \cos(2\pi nf_\circ T_s k) + b_n \sin(2\pi nf_\circ T_s k)\right] \quad (2)$$

This equation calculates the values of x_0, $f_\circ$, a_n, and b_n (for n= 1,…, N).

The phase and magnitude in each harmonic can be calculated using these formulas [11]:

$$\begin{cases} A_n(t) = \sqrt{a_n^2(t) + b_n^2(t)} \\ \varphi_n(t) = \begin{cases} \tan^{-1}(a_n(t)/b_n(t)) & ;b_n(t) \geq 0 \\ \pi + \tan^{-1}(a_n(t)/b_n(t)) & ;b_n(t) \leq 0 \end{cases} \end{cases} \quad \textbf{(3)}$$

However, previous calculations require the signal frequency to be known. In this method, signal frequency is initially determined by the proposed algebraic method by detecting its zero crossings for the first period.

The DC value, magnitude, and the phase of harmonics can then be calculated based on the signal samples. The parameters of $\cos(2\pi nf_\circ T_s k)$ and $\sin(2\pi nf_\circ T_s k)$ are revealed when the values of $f_\circ, k$ and $x(k)$ are known.

The values of x_0, a_n and b_n should be determined. 2N+1 unknowns were observed, where N is the number of the last harmonic in $x(t)$. The variables $\cos(2\pi nf_\circ T_s k)$ and $\sin(2\pi nf_\circ T_s k)$ are known. Therefore, the equation can be considered as a linear equation because its variables are x_0, a_n and b_n.

Accordingly, the 2N+1 linear equations with 2N+1 unknowns for the 2N+1 samples of x(t) can be obtained using the following formulation:

$$X = AY \quad (4)$$

$X = [x(1)\,x(2)...x(M)]^T$, $Y = [x_0\,a_1...a_n\,b_1...b_n]^T$,

$x(k) = x(T_s k), (for\ k = 1,...,M)$

where, M=N+1 and $A = [A_1, A_2]$ and

$$A_1 = \begin{bmatrix} 1\cos(2\pi f_\circ(1T_s))...\cos(2\pi Nf_\circ(1T_s)) \\ 1\cos(2\pi f_\circ(2T_s))...\cos(2\pi Nf_\circ(2T_s)) \\ \vdots \\ 1\cos(2\pi f_\circ(MT_s))...\cos(2\pi Nf_\circ(MT_s)) \end{bmatrix}_{2N+1,N+1}$$

$$A2 = \begin{bmatrix} \sin(2\pi f_\circ(1T_s))...\sin(2\pi Nf_\circ(1T_s)) \\ \sin(2\pi f_\circ(2T_s))...\sin(2\pi Nf_\circ(2T_s)) \\ \vdots \\ \sin(2\pi f_\circ(MT_s))...\sin(2\pi Nf_\circ(MT_s)) \end{bmatrix}_{2N+1,N}$$

To solve Y the following equation is used:

$$Y = A^{-1}X \quad (5)$$

A^{-1} must be calculated. However, A-1 is constant because A is a matrix with constant terms. Therefore, A can be calculated once. The calculation of A^{-1} can be used to solve the above equation. A^{-1} is a 2N+1 of the 2N+1 matrix, which can be written as:

$$A^{-1} = [c_{ij}]_{2N+1,2N+1}, (i, j = 1,...,2N+1) \quad (6)$$

Based on (5) and (6), the following equation can be derived as:

$$x_0 = \sum_{j=1}^{2N+1} c_{1,j}.x(j) \quad (7)$$

$$a_n = \sum_{j=1}^{2N+1} c_{n+1,j}.x(j) \quad (8)$$

$$b_n = \sum_{j=1}^{2N+1} c_{N+n+1,j}.x(j) \quad (9)$$

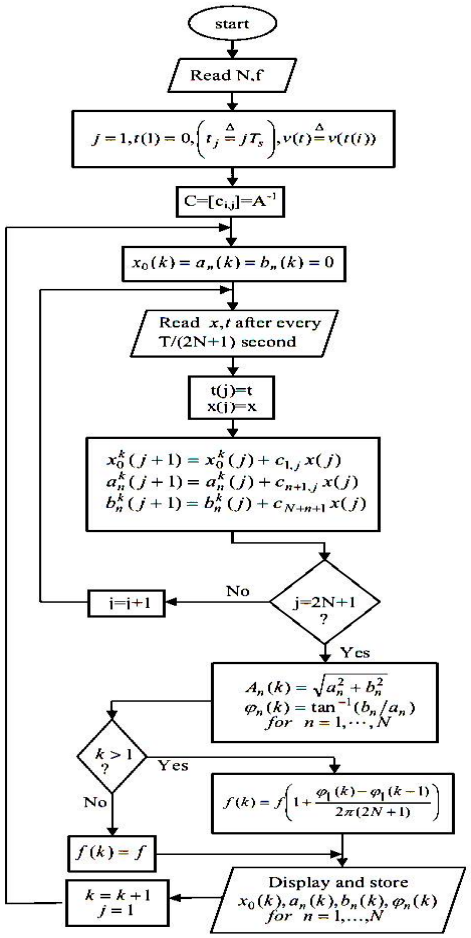

Fig. 3. Flowchart of the proposed recursive algebraic algorithm for harmonic calculation

One period of signal monitoring is needed to calculate x_0, a_n and b_n. The summation and multiplication operations of 2N+1 are also required for this calculation. This calculation procedure is conducted among the samples. The method for k[th] cycle is expressed as:

$$\begin{aligned} x_0^k(j+1) &= x_0^k(j) + c_{1,j}\,x(j) \\ a_n^k(j+1) &= a_n^k(j) + c_{n+1,j}\,x(j) \\ b_n^k(j+1) &= b_n^k(j) + c_{N+n+1}\,x(j) \end{aligned} \tag{10}$$

Where N is the last harmonic, n is the number of harmonics, k is the number of cycles, and j is the number of samples in the k[th] cycle.

The initial value of any variable is zero at the beginning of any period, and the number of samples in any period starts from one, which is rendered as: $x_0^k(1)=a_n^k(1)=b_n^k(1)=0$. Thus, the DC values and harmonics are calculated after the 2N+1 sample at one period. Then, one is added to k, and *j* becomes zero again until the DC values and harmonics are calculated for the $(k+1)$ [th] period.

This method is recursive because the variables are calculated based on their values in the previous stage at any sampling stage in a given cycle. Fig. 3 shows the flowchart of the algorithm for the recursive algebraic method.

4. CALCULATION OF THE REFERENCE CURRENT

4.1. Instantaneous active and reactive p-q power theory

The instantaneous active and reactive p-q power theory is also known as the instantaneous power theory or p-q theory [12]. In instantaneous power theory, three-phase currents (i_{La}, i_{Lb}, i_{Lc}) and voltages (v_{sa}, v_{sb}, v_{sc}) in the a–b–c coordinates are algebraically transformed to the α–β coordinates using Clarke's transformation, as shown in the following equations [13]:

$$\begin{bmatrix} v_\alpha \\ v_\beta \end{bmatrix} = \sqrt{\frac{2}{3}} \begin{bmatrix} 1 & -1/2 & -1/2 \\ 0 & \sqrt{3}/2 & -\sqrt{3}/2 \end{bmatrix} \begin{bmatrix} v_{sa} \\ v_{sb} \\ v_{sc} \end{bmatrix} \tag{11}$$

$$\begin{bmatrix} i_\alpha \\ i_\beta \end{bmatrix} = \sqrt{\frac{2}{3}} \begin{bmatrix} 1 & -1/2 & -1/2 \\ 0 & \sqrt{3}/2 & -\sqrt{3}/2 \end{bmatrix} \begin{bmatrix} i_{La} \\ i_{Lb} \\ i_{Lc} \end{bmatrix} \tag{12}$$

The instantaneous power is then calculated as follows:

$$\begin{bmatrix} p \\ q \end{bmatrix} = \begin{bmatrix} v_\alpha & v_\beta \\ v_{-\beta} & v_\alpha \end{bmatrix} \begin{bmatrix} i_\alpha \\ i_\beta \end{bmatrix} \tag{13}$$

$$p = \bar{p} + \tilde{p}, \; q = \bar{q} + \tilde{q} \tag{14}$$

The entire reactive power and AC component of the active power are used as the reference power to obtain a sinusoidal current with unity power factor. The reference currents in a–ß coordinates are calculated as follows:

$$\begin{bmatrix} i_\alpha^{'} \\ i_\beta^{'} \end{bmatrix} = \frac{1}{v_\alpha^2 + v_\beta^2} \begin{bmatrix} v_\alpha & -v_\beta \\ v_\beta & v_\alpha \end{bmatrix} \begin{bmatrix} -\tilde{p} + \bar{p}_{loss} \\ -q \end{bmatrix} \quad (15)$$

Here, $\bar{p}_{loss}$ is the average value of losses in the inverter, which is obtained from the voltage regulator. The DC-link voltage regulator is designed to provide good compensation and excellent transient response. The actual DC-link capacitor voltage (V_{dc}) is measured by reference value (V_{dc}^*), and the error is processed by IT2FLC. The inputs of the IT2FLC are the capacitor voltage deviation and its derivative, whereas its output is the real power $\bar{p}_{loss}$ requirement for voltage regulation. The reference current is calculated as shown in Eq. 17:

$$\begin{bmatrix} i_{sa}^* \\ i_{sb}^* \\ i_{sc}^* \end{bmatrix} = \sqrt{\frac{2}{3}} \begin{bmatrix} 1 & 0 \\ -1/2 & \sqrt{3}/2 \\ -1/2 & -\sqrt{3}/2 \end{bmatrix} \begin{bmatrix} i_\alpha^{'} \\ i_\beta^{'} \end{bmatrix} \quad (16)$$

$$\begin{bmatrix} i_{fa}^* \\ i_{fb}^* \\ i_{fc}^* \end{bmatrix} = \begin{bmatrix} i_{La} - i_{sa}^* \\ i_{Lb} - i_{sb}^* \\ i_{Lc} - i_{sc}^* \end{bmatrix} \quad (17)$$

This control algorithm is illustrated in Fig. 4.

4.2. The proposed method

The source voltage should be a pure sinusoidal wave given as:

$$v_s(t) = V_p \sin(\omega t) \quad (18)$$

The nonlinear load current is represented as:

$$\begin{aligned} i(t) &= \sum_{n=1}^{\infty} I_n \sin(n\omega t + \theta_n) \\ &= I_1 \sin(\omega t + \theta_1) + \sum_{n=2}^{\infty} I_n \sin(n\omega t + \theta_n) \\ &= I_1 \cos\theta_1 \sin(\omega t) + I_1 \sin\theta_1 \cos(\omega t) \\ &+ \sum_{n=2}^{\infty} I_n \sin(n\omega t + \theta_n) \\ &= i_{1p}(t) + i_{1q}(t) + i_h(t) \end{aligned} \quad (19)$$

where I_n, θ_n is the peak value of amplitude and the phase angle of the n-order harmonic current, respectively; n is a positive integer; I_1, θ_1 is the peak value of the amplitude and the phase angle of the fundamental current, respectively; $i_{1p}(t)$ is the component of the fundamental active current; $i_{1q}(t)$ is the component of the fundamental reactive current; and $i_h(t)$ is the component of the harmonics current.

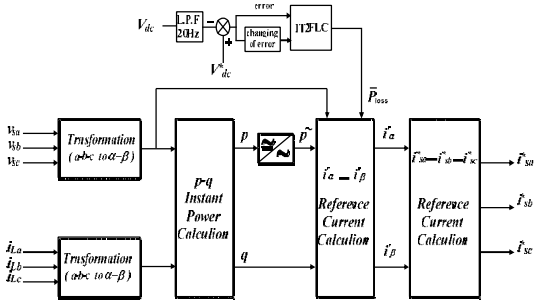

Fig. 4. Reference current extraction with conventional p-q theory using IT2FLC

A signal with unity amplitude is obtained from the source voltage using as the following equation:

$$u(t) \quad \sin(\omega t) \quad (20)$$

By using the Fourier algorithm, the amplitude of the active component of the

fundamental load current can be determined as:

$$I^*_{smp} = \frac{2}{T}\int_0^T i_L(t).u(t)d(t)$$

$$I^*_{smp} = \frac{2}{T}\int_0^T [I_1\cos\theta_1\sin(\omega t) + I_1\sin\theta_1\cos(\omega t) + \sum_{n=2}^{\infty} I_n\sin(n\omega t+\theta_n)]\sin(\omega t)dt$$

$$= \frac{2}{T}\int_0^T [I_1\cos\theta_1\sin^2(\omega t) + I_1\sin\theta_1\cos(\omega t)\sin(\omega t) + \sum_{n=2}^{\infty} I_n\sin(n\omega t+\theta_n).\sin(\omega t)]dt$$

$$= \frac{2}{T}\int_0^T [I_1\cos\theta_1(\frac{1-\cos(2\omega t)}{2}) + I_1\sin\theta_1\frac{\sin(2\omega t)}{2} + \sum_{n=2}^{\infty}\frac{I_n}{2}\{-\cos[(n+1)\omega t+\theta_n]+\cos[(n-1)\omega t+\theta_n]\}]dt$$

$$= I_1\cos\theta_1 = I^*_{smp} \quad (21)$$

In this method, the peak value of the amplitude and the phase angle of the fundamental load current (I_1, θ_1) from a recursive algebraic approach block are first obtained before calculating the displacement power factor $(\cos\theta_1)$. Fig. 5 shows the schematic diagram of the $I.\cos\Phi$ based on a recursive algebraic approach control algorithm.

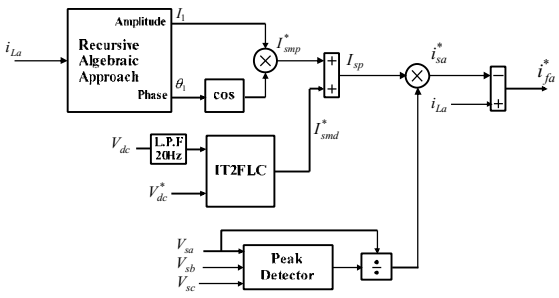

Fig. 5. Reference current extraction

In addition to the real power of the load the extra power losses in the inverter and the capacitor leakage can be calculated by the voltage fluctuations at the DC bus capacitor. The corresponding current amplitude (I^*_{smd}) is calculated using an interval type2 fuzzy logic controller. The voltage of DC side capacitor (V_{dc}) is sensed and passed through Butterworth design based LPF with a cut off frequency of 20 Hz then compared with a reference value (V^*_{dc}). The obtained errors are:

$$e(n) = V^*_{dc}(n) - V_{dc}(n) \quad (22)$$

$$ce(n) = e(n) - e(n-1) \quad (23)$$

at the n^{th} sampling instant are used as the inputs for type2 fuzzy processing. The output of the type2 fuzzy controller is considered as the current amplitude I^*_{smd}.

This current amplitude is added to the amplitude of the active component of the fundamental load current in each phase $(I_1\cos\theta_1)$. Therefore, the three-phase source provides the losses in the active filter, and enables the active filter DC bus to become self-supporting [14].

The following equations provide the reference source current, i_f:

$$I_{sp} = I^*_{smp} + I^*_{smd} \quad (24)$$

$$i^*_s(t) = I_{sp}\sin(\omega t) \quad (25)$$

$$i^*_f(t) = i_L(t) - i^*_s(t) \quad (26)$$

5. INTERVAL TYPE-2 FUZZY LOGIC BASED DC BUS VOLTAGE CONTROLLER

While precise knowledge of the system model is not available, FLC's are a superior choice. The inputs of the FLC are the capacitor voltage deviation and its derivative and the output of the FLC is the

real power requirement for voltage regulation as shown in Fig.4. In this paper first, a type-1FLC is modeled and then the same configuration is chosen for the design of IT2 FLC.

For type-1FLC, the following seven fuzzy levels or sets are chosen, to convert the inputs and output variables into linguistic variables as: NB (negative big), NM (negative medium), NS (negative small), ZE (zero), PS (positive small), PM (positive medium), and PB (positive big) are chosen [13]. Membership functions (MFs) selected here for the inputs and output variables are shown in Figs 6, 7.

On the basis of the theory that in the steady state, small errors require fine control, which needs fine input/output variables and in the transient state, large errors require coarse control, which needs coarse input/output variables; rule base elements of the table are determined. Whereas both inputs have seven subsets, the elements of the rule table as shown in Table 1 are obtained [15]. The T2FLC was first introduced by Zadeh in 1970s, as an extension of the type-1 fuzzy controller [16].

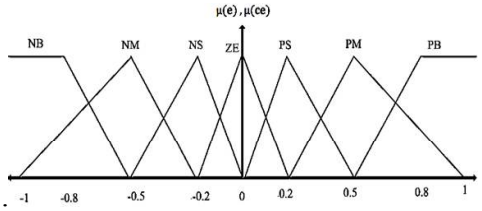

Fig. 6. Inputs normalized membership function

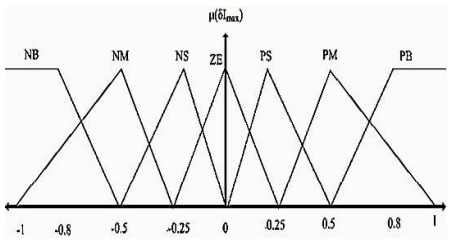

Fig. 7. Output normalized membership function

Table 1. Fuzzy control rule

changing of error c(ce) \ error (e)	NB	NM	NS	ZE	PS	PM	PB
NB	NB	NB	NB	NB	NM	NS	ZE
NM	NB	NB	NB	NM	NS	ZE	PS
NP	NB	NB	NM	NS	ZE	PS	PM
ZE	NB	NM	NS	ZE	PS	PM	PB
PS	NM	NS	ZE	PS	PM	PB	PB
PM	NS	ZE	PS	PM	PB	PB	PB
PB	ZE	PS	PM	PB	PB	PB	PB

As shown in Fig 8, similar to the structure of the conventional type-1 FLC, the type-2 fuzzy logic controller (T2FLC) also contains the components; fuzzifier, rule base, fuzzy inference engine and output processor which comprises of type-reducer and defuzzifier while for a type-1 fuzzy is just a defuzzifier.

The type reducer maps a type2 FLS set into a type-1 fuzzy set and defuzzifier as like as type-1 transforms a fuzzy output into a crisp output.

In the type-2 fuzzy set, the membership grade for each element is also a fuzzy set in 0 - 1, unlike the type-1 fuzzy set whose membership grade is a crisp number of either 0 or 1. The membership functions of type-2 fuzzy sets are three dimensional and include a footprint of uncertainty, as can be seen by the shaded region bounded by the lower and upper membership functions, both of which are type-1 MFs as shown in Fig 9. Normally, the T2FLC has characteristics of profound computation due to heavy computational load at the step of type reducing process.

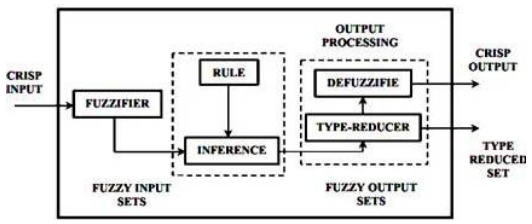

Fig. 8. Type-2 fuzzy logic controller

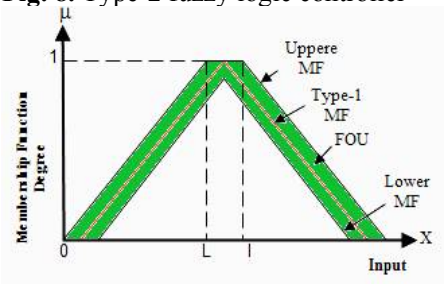

Fig. 9. Membership function of IT2FLC

A footprint of uncertainty (FOU) which displays the uncertainties in the shape and position of the type-1 fuzzy set provides an additional degree of freedom to handle uncertainties. The T2FLC can be used at the uncertain circumstances when the membership grades cannot be determined exactly [17]. To simplify the computation, the secondary membership functions can be set to either 0 or 1 so as to derive the interval T2FLC [18]. Suppose that there are M rules in the rule base, each of which has the following form

Rule k : IF x_1 is $\tilde{A}_1^k$ and x_2 is $\tilde{A}_2^k$ and …… and x_p is $\tilde{A}_p^k$,THEN y is $\left[\underline{w}^k, \overline{w}^k\right]$.

where k = 1,2,…M , p is the number of input variables in the antecedent part, $\tilde{A}_i^k$ (i= 1,2,…,p , k=1,2,…,M) and $\underline{w}^k, \overline{w}^k$ are the singleton lower and upper weighting factors of the THEN-part. Once a crisp input $X = (x_1, x_2, ..., x_p)^T$ is applied to the interval T2FLC, through the singleton fuzzifier and the inference process, the firing strength of the k[th] rule which is an interval type-1 set can be obtained as $F^k = \left[\underline{f}^k, \overline{f}^k\right]$, in which:

$$\underline{f}^k = \underline{\mu}_{\tilde{A}_1^k}(x_1) * \underline{\mu}_{\tilde{A}_2^k}(x_2) * ... * \underline{\mu}_{\tilde{A}_p^k}(x_p) \quad (27)$$

$$\underline{f}^k = \underline{\mu}_{\tilde{A}_1^k}(x_1) * \underline{\mu}_{\tilde{A}_2^k}(x_2) * ... * \underline{\mu}_{\tilde{A}_p^k}(x_p) \quad (28)$$

$$\overline{f}^k = \overline{\mu}_{\tilde{A}_1^k}(x_1) * \overline{\mu}_{\tilde{A}_2^k}(x_2) * ... * \overline{\mu}_{\tilde{A}_p^k}(x_p) \quad (29)$$

Where $\underline{\mu}(\,)$ and $\overline{\mu}(\,)$ denote the grades of the lower and upper membership functions of interval T2FLC and * denotes minimum or product t-norm.

The outputs of the inference engine should be type reduced and then defuzzified so as to create a crisp output. For design of the interval T2FLC for the DC voltage regulator, the same configuration as that of the conventional type-1FLC is used (Figs. 6 and 7). There are two inputs (error and rate of error) and single output in which each set of input /output variables has similar seven linguistic variables. The fuzzy labels are negative big (NB), negative medium (NM), negative small (NS), zero (Z), positive small (PS), positive medium (PM), positive big (PB). The rules for interval T2FLC are also similar to the type 1 FLC but their antecedents and consequents are represented by the interval T2FLC. The diagonal rule table as summarized in Table 1 is constructed for the scenario in which error and change of error approach zero with a fast rise time and without overshoot. Here, the Mamdani interval T2FLC is considered and the popular center-of-sets is assigned for type-reduction method. The Karnik-Mendel algorithm is then used to obtain the type reduced set.

Here, after writing required m-codes in MATLAB for IT2FLC, Embedded MATLAB Function Block is used to incorporate into the Simulink model. The

capacitor voltage deviation $e(n)$ and its derivative $ce(n)$ are fed to the embedded MATLAB function as the inputs and the output is the real power requirement for voltage regulation.

6. ADAPTIVE-HYSTERESIS CURRENT CONTROLLER

The PWM -voltage source inverter's voltage and current waves for phase A is shown in Fig. 10.

At point 1, when current crosses the lower hysteresis band, the transistor T1 will be switched-on. The inverter output voltage and the current will rise. In the same way, when the current touches the upper band limit at point 2 then the inverter output voltage and consequently the current will start decaying, by switch-on the transistor T4. Using the Fig. 10, the following equations can be written for the switching interval t1and t2 [19].

$$\frac{di_{fa}^{+}}{dt}=\frac{1}{L}(0.5V_{dc}-V_s) \quad (30)$$

$$\frac{di_{fa}^{-}}{dt}=-\frac{1}{L}(0.5V_{dc}+V_s) \quad (31)$$

where L = inductance of phase; di_{fa}^{+} and di_{fa}^{-} are the rising and falling current segments, respectively.

From the geometry of Fig. 10 can be written:

$$\frac{di_{fa}^{+}}{dt}t_1-\frac{di_{fa}^{*}}{dt}t_1=2HB \quad (32)$$

$$\frac{di_{fa}^{-}}{dt}t_2-\frac{di_{fa}^{*}}{dt}t_2=-2HB \quad (33)$$

$$t_1+t_2=T_c=\frac{1}{f_c} \quad (34)$$

Where t_1 and t_2 are the respective switching intervals and f_c is the switching frequency. Adding (32) and (33) and substituting (34), it can be written:

$$t_1\frac{di_{fa}^{+}}{dt}+t_2\frac{di_{fa}^{-}}{dt}-\frac{1}{f_c}\frac{di_{fa}^{*}}{dt}=0 \quad (35)$$

Subtracting (33) from (32), so:

$$t_1\frac{di_{fa}^{+}}{dt}-t_2\frac{di_{fa}^{-}}{dt}-(t_1-t_2)\frac{di_{fa}^{*}}{dt}=4HB \quad (36)$$

Substituting (35) in (36), gives:

$$(t_1+t_2)\frac{di_{fa}^{+}}{dt}-(t_1-t_2)\frac{di_{fa}^{*}}{dt}=4HB \quad (37)$$

Substituting (31) in (35) and after simplifying:

$$t_1-t_2=\left(\frac{di_{fa}^{*}}{dt}\right)\Big/ f_c\left(\frac{di_{fa}^{+}}{dt}\right) \quad (38)$$

Finally, Substituting (38) in (37), it gives:

$$HB=\left\{\frac{0.125V_{dc}}{Lf_c}\left[1-\frac{4L^2}{V_{dc}^2}\left(\frac{v_s}{L}+m\right)^2\right]\right\} \quad (39)$$

Hence f_c is frequency of modulation, $m=\frac{di_{fa}^{*}}{dt}$ is the slope of command current wave, L is coupling inductance and V_{dc} is the DC link capacitor voltage. To control the switching pattern of the inverter, hysteresis band (HB) can be modulated at different points of fundamental frequency cycle. In order to have symmetrical operation of all three phases, it is required that the hysteresis bandwidth (HB) profiles HBa, HBb and HBc will be same, but have

difference in phase. As the equation 39 demonstrates, the hysteresis bandwidth HB as a function of supply voltage, dc link voltage and reference current variations (m) can be modulated to minimize the effects of current distortion on modulated waveform. Therewith the modulation frequency is kept almost constant; the performance of PWM and shunt Active Power Filter substantially is improved. Fig.11 shows block diagram of the adaptive hysteresis bandwidth computation for phase (A).

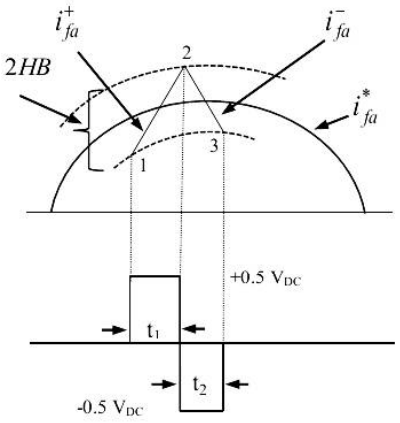

Fig. 10. Adaptive hysteresis current controller

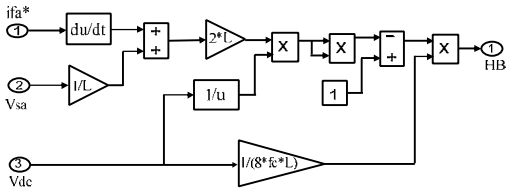

Fig. 11. Block diagram of the adaptive hysteresis bandwidth computation

7. SIMULATION RESULTS

The simulations conducted on the test system are shown in Fig. 12 to evaluate the performance of the SAPFs using the $I\cos\Phi$ algorithm based on a recursive algebraic approach for generating the reference compensating currents. The test system comprises three-phase voltage source, SAPF, and an uncontrolled rectifier with R and L loads. An inductor, L_f and resistor, R_f were used to connect SAPF to the test system. The system parameters are given in Table 2.

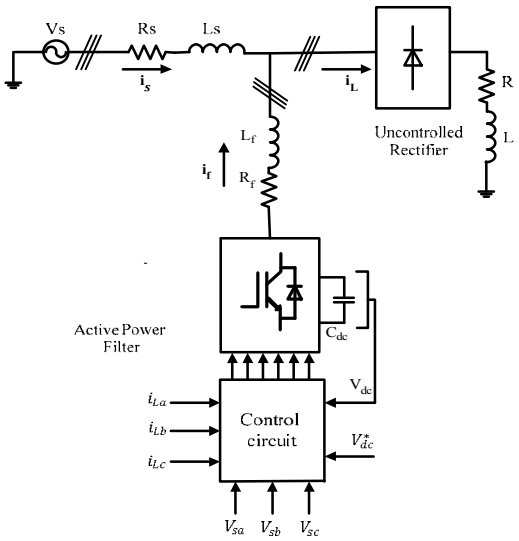

Fig. 12. Test power system

Table 2. Circuit parameters of SAPF

Parameter Names	Numerical Value
Source Voltage	312 V (peak) , 50 Hz
Source Resistance and Inductance	0.1 ohm , 1 mH
Filter Inductance and Resistance	1mH , 0.1 ohm
Load Resistance and Inductance	5 Ω , 1 mH
DC Capacitor	2500 µF
DC Capacitor Reference Voltage	650V
Sample Time (Ts)	7.14 e-6

Table 2 shows the circuit parameters used in the simulation while Table 3 shows the values of total harmonic distortion in percent (%), power factor, and reactive power measured at the PCC. Figure 13 show the source currents without SAPF while Figures 14 and 15 show the source currents after compensation using the p-q

theory and the proposed reference current generation using the recursive algebraic approach, respectively.

Table 3. Total harmonic distortion in percent (%), power factor and reactive power

Method used	Source Current (phase a)	Power Factor	Reactive Power (Var)
Before any shunt compensation	22.10	0.9537	4838
With recursive algebraic approach	2. 66	1	17.29
With p-q theory	2.97	1	76.21

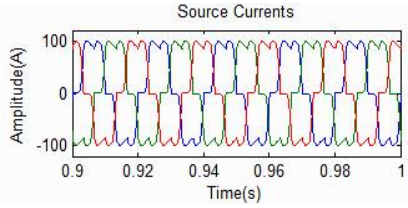

Fig. 13. Source currents without SAPF

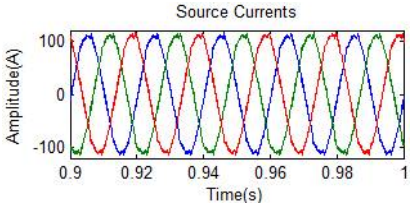

Fig. 14. Source currents for SAPF with PQ theory

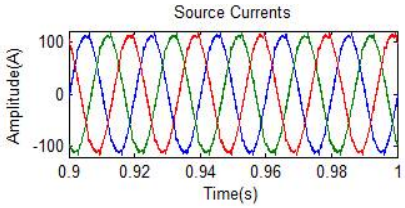

Fig. 15. Source currents for SAPF using the proposed method

Comparison among Figs. 13, 14 and 15 indicates that the source currents consist of fundamental current only, and the network with SAPF has fewer harmonic than the network without SAPF. Table 3 suggests that the harmonic and reactive currents are greatly reduced after compensation. The SAPF result with the reference current generation based on the recursive algebraic approach is better than SAPF with the generation system based on the p-q theory.

8. CONCLUSIONS

This paper presents a novel technique to generate the reference current for a three-phase SAPF with nonlinear loads. SAPF was simulated and its performance was analyzed in a sample power system. The results of the simulation on the test system prove that the injected harmonics are significantly reduced and power factor is improved by using the proposed algorithm based on the recursive algebraic approach. Compared with the p-q theory, the proposed approach is more effective in reducing reactive and THD to less than 3%.

REFERENCES

[1] A. Bhattacharya, C. Chakraborty, "A shunt active power filter with enhanced performance using ANN-based predictive and adaptive controllers," IEEE Trans. Ind. Electron., vol. 58, no. 2, pp. 421–428,Feb. 2011.

[2] S. Rahmani, N. Mendalek, and K. Al-Haddad, "Experimental design of a nonlinear control technique for three-phase shunt active power filter,"IEEE Trans. Ind. Electron., vol. 57, no. 10, pp. 3364–3375, Oct. 2010.

[3] S.H. Fathi, M. Pishvaei, and G.B. Gharehpetian, "A frequency domain method for instantaneous determination of reference current in shunt active filter," TENCON, IEEE Region 10 Conference,1-4, 2006.

[4] Z. Salam, P. C. Tan, and A. Jusoh, "Harmonics mitigation using active power filter: A technological review," Elektrika Journal of Electrical Engineering, 8: 17-26, 2006.

[5] T. Komrska, J. Zák, and Z. Peroutka,"Control strategy of active power filter with adaptive FIR filter-based and DFT-based reference estimation," Power Electronics Electrical

Drives Automation and Motion (SPEEDAM), 2010 International Symposium on, Page(s): 1524 – 1529, 2010.

[6] G. Chen, Y. Jiang, and H. Zhou, "Practical Issues of Recursive DFT in Active Power Filter Based on CPC Power Theory, "Power and Energy Engineering Conference, APPEEC 2009. Asia-Pacific, Page(s): 1 – 5, 2009.

[7] H. Akagi, Yoshihira Kanazawa, and Akira Nabae,"Instantaneous Reactive Power Compensators Comprising Switching Devices Without Energy Storage Components, " IEEE Transactions On Industry Applications, Vol. IA20, No.3, May/June1998.

[8] M.A Kabir, U. Mahbub," Synchronous Detection and Digital control of Shunt Active Power Filter in Power Quality Improvement," IEEE Power and Energy Conference at Illinois (IEEE PECI), University of Illinois at Urbana-Champaign, USA, 2011.

[9] A. Khoshkbar Sadigh, M. Farasat, S.M. Barakati,"Active power filter with new compensation principle based on synchronous reference frame," North America Power Symposium (NAPS),DOI: 10.1109/NAPS.2009.5484077,2009.

[10] B.S. Kumar, K.R. Reddy, V. Lalitha,"PI, fuzzy logic controlled shunt active power filter for three-phase four-wire systems with balanced, unbalanced and variable loads," Journal of Theoretical and Applied Information Technology 23 (2), pp. 122-130 0 ,2011.

[11] A. Peiravi, R. Ildarabadi ,"Recursive algebraic method of computing power system harmonics," IEEJ Transactions on Electrical and Electronic Engineering Volume 6, Issue 4, pages 338–344, July 2011.

[12] B. Berbaoui , C.Benachaiba,"Power Quality Enhancement using Shunt Active Power Filter Based on Particle Swarm Optimization," Journal of Applied Sciences, 11: 3725-3731, 2011.

[13] H.Akagi, Y.Kanazawa and N.Nabae,"Generalized theory of the instantaneous reactive power in three-phase circuits", in Proc. Int. Power El. Conf., pp 1375-1386, Tokyo, Japan, 1983

[14] G. Bhuvaneswari, M.G. Nair, "Design, Simulation, and Analog Circuit Implementation of a Three-Phase Shunt Active Filter Using the $I\cos\varphi$ Algorithm," Power Delivery, IEEE Transactions on, Volume23, Issue: 2, Page(s): 1222 – 1235, 2008.

[15] P. Karuppanan , K. K. Mahapatra , "PLL with PI, PID and Fuzzy Logic Controllers based Shunt Active Power Line Conditioners," IEEE International Conference on Power Electronics, Drives and Energy Systems-Dec 21 o 23, 2010.

[16] L. A. Zadeh, "The concept of a linguistic variable and its application to approximate reasoning-1," Inf. Sci., vol. 8, pp. 199-249, 1975.

[17] J.M. Mendel, Uncertain Rule-Based Fuzzy Logic: Introduction and new directions, Prentice Hall, USA, (2000).

[18] J.M. Mendel, R.I. John and F. Liu, " Interval type-2 fuzzy logic systems made simple", IEEE Trans. Fuzzy Syst., 14: 808-821. 2006.

[19] P . Karuppanan , K. K. Mahapatra , "PI and fuzzy logic controllers for shunt active power filter — A report," ISA Transactions vol. 51 issue 1 January, p. 163-169, 2012.